/
_/_ _ _ -_/.

_63/599_

Final Report to the

NATIONAL AERONAUTICS AND SPACE ADMINISTRATION
on Research Supported by Grant NAG3-1389:

Phase Segregation Due to
Simultaneous Migration and Coalescence

Name and Address of Institution:

The Regents of the
University of Colorado
Campus Box 19
Boulder, CO 80309-0019
(Educational Institution)

Time Period of Support:

12/1/92-12/31/96

Amount Provided by NASA:

$120,000

Principal Investigator:

Robert H. Davis, Professor
Department of Chemical Engineering
Campus Box 424
University of Colorado
Boulder, Colorado 80309-0424
(303) 492-7314 voice
(303) 492-4341 fax

Responsible NASA Official:

R. Balasubramaniam
Mail Stop 500-217
NASA Lewis Research Center
210000 Brookpark Road
Cleveland, Ohio 44135
(216) 433-2878 voice
(216) 433-8660 FAX

Robert H. Davis
Principal Investigator

Objectives

The primary objective of the research was to perform ground-based analysis and experiments on the interaction and coalescence of spherical drops (or bubbles), leading to macroscopic phase separation (Figure 1). Migration of the drops occurs as a result of the individual and collective action of gravity and thermocapillary effects. Larger drops migrate faster than smaller ones, leading to the possibility of collisions and coalescence. Very small drops also undergo Brownian motion, which also may lead to collisions and coalescence.

Accomplishments

The population dynamics equations for homogeneous dispersions having no spatial variation or phase separation were solved for droplet growth due to the separate effects of Brownian, gravitational and thermocapillary motion and coalescence (Wang & Davis, 1993) and due to the combined effects of thermocapillary and gravitational motion and coalescence (Zhang et al., 1993). Included among the key results are the discoveries of *thermocapillary repulsion*, in which a highly conducting small drop will move faster than a nearby larger drop, thereby preventing coalescence, and of a *collision-forbidden region*, which occurs for antiparallel alignment of the temperature gradient and gravity vector due to the different dependencies of gravitational and thermocapillary relative motion on the separation distance of two drops or bubbles.

A theoretical analysis was performed (Wang & Davis, 1995) for nonhomogeneous dispersions undergoing simultaneous phase separation and drop motion and coalescence due to gravity. The average drop size and rate of phase separation initially increase due to coalescence, and then decrease due to the larger drops moving out of the suspension (Figures 2 and 3). The volume fraction of the dispersed phase continuously decreases, as the drops rise or settle out of the dispersion (Figure 4). A key dimensionless parameter, $N_\tau = \tau_s/\tau_c$, representing the ratio of sedimentation and coalescence time scales, governs the process. Larger values of this parameter indicate more coalescence.

Experiments to observe drop coalescence and phase segregation due to gravity were performed with 1,2-propanediol drops in dibutyl sebacate and with an aqueous biphase mixture of 1% dextran and 6.5% polyethylene glycol by weight (Davis et al., 1994; Wang & Davis, 1996b) As seen in Figure 5-7, the results are in good agreement with the theory and have been used to infer values for the composite Hamaker constant, which represents the strength of the attractive van der Waals forces.

Studies to predict the collective effects of Brownian diffusion and gravitational or convective motion on drop coalescence rates were also performed (Wang et al., 1994; Zinchenko & Davis, 1994, 1995; Wang & Davis, 1996a). It was found that the synergistic coalescence rates are higher than the individual coalescence rates added together (Figure 8).

Theoretical work on the effects of drop deformation on the interaction and coalescence of two drops in buoyancy-driven motion was also initiated. An asymptotic theory predicts that small deformations inhibit coalescence (Rother et al., 1997). Thus, an attractive van der Waals force is necessary for coalescence. A fully three-dimensional, boundary-integral numerical method has been developed for large deformations (Zinchenko et al., 1997). Drops with moderate or large viscosity are predicted to elongate and break during the interaction (Figure 9), while bubbles tend to align and eventually coalesce (Figure 10). Related work was also undertaken on the interaction of two deformable drops in axisymmetric thermocapillary motion (Zhou & Davis, 1996).

Publications

Davis, R.H., Wang, H. & Hawker, D. 1994 Phase segregation due to simultaneous migration and coalescence. *Second Microgravity Fluid Physics* Conference (NASA Conf. Pub. 3276), 101-106.

Loewenberg, M. & Davis, R.H. 1994 Flotation rates of fine spherical particles and droplets. *Chem. Eng. Sci.* **49**, 3923-3941.

Rother, M.A., Zinchenko, A.Z. & Davis, R.H. 1997 Buoyancy-driven coalescence of slightly deformable drops. *J. Fluid Mech.* (under review).

Wang, H. 1994 *Modeling and Experimental Studies of Drop Coalescence and Phase Separation*, Ph.D. Thesis, U. Colorado.

Wang, H. & Davis, R.H. 1993 Droplet growth due to Brownian, gravitational, or thermocapillary motion and coalescence in dilute dispersions. *J. Colloid Inerf. Sci.* **159**, 108-118.

Wang, H. & Davis, R.H. 1995 Simultaneous sedimentation and coalescence of a dilute dispersion of small drops. *J. Fluid Mech.* **295**, 247-261.

Wang, H. & Davis, R.H. 1996a Collective effects of gravitational and Brownian coalescence on droplet growth. *J. Colloid Interf. Sci.* **178**, 47-52.

Wang, H. & Davis, R.H. 1996 Experiments on phase separation of dilute dispersions of coalescing drops. *J. Colloid Interf. Sci.* **181**, 93-98.

Wang, H., Zinchenko, A.Z. & Davis, R.H. 1994 The collision rate of small drops in linear flow fields. *J. Fluid Mech.* **265**, 161-188.

Zhang, X., Wang, H. & Davis, R.H. 1993 Collective effects of temperature gradients and gravity on droplet coalescence. *Phys. Fluids A* **5**, 1602-1613.

Zhou, H. & Davis, R.H. 1996 Axisymmetric thermocapillary migration of two deformable viscous drops, *J. Colloid Interf. Sci.* **181**, 60-72.

Zinchenko, A.Z. & Davis, R.H. 1994 Gravity-induced coalescence of drops at arbitrary Péclet numbers. *J. Fluid Mech.* **280**, 119-148.

Zinchenko, A.Z. & Davis, R.H. 1995 Collision efficiency of drops and solid spheres in a shear flow at arbitrary Péclet numbers. *Phys. Fluids* **7**, 2310-2327.

Zinchenko, A.Z., Rother, M.A. & Davis, R.H. 1997 A novel boundary-integral algorithm for viscous interactions of deformable drops. *Phys. Fluids* (in press).
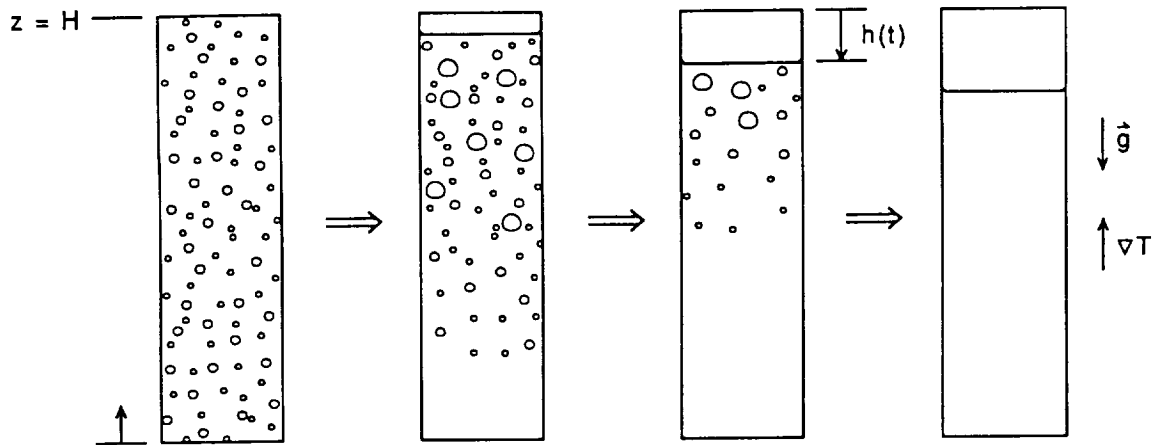
Fig. 1 - Schematic of the time evolution of the phase separation process due to the simultaneous migration and coalescence of rising drops or bubbles.
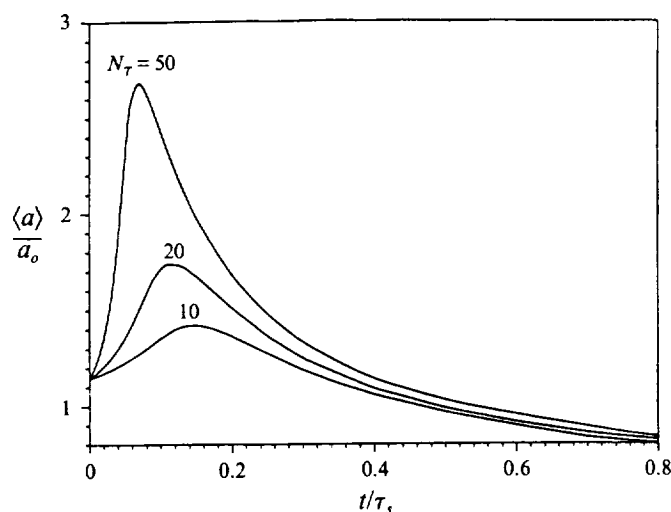

Fig. 2 - Predicted time evolution of the average drop radius at height $z/H = 0.5$ for a dispersion having viscosity ratio $\hat{\mu} = 0.1$, and initial dimensionless standard deviation $\hat{\sigma} = 0.2$.
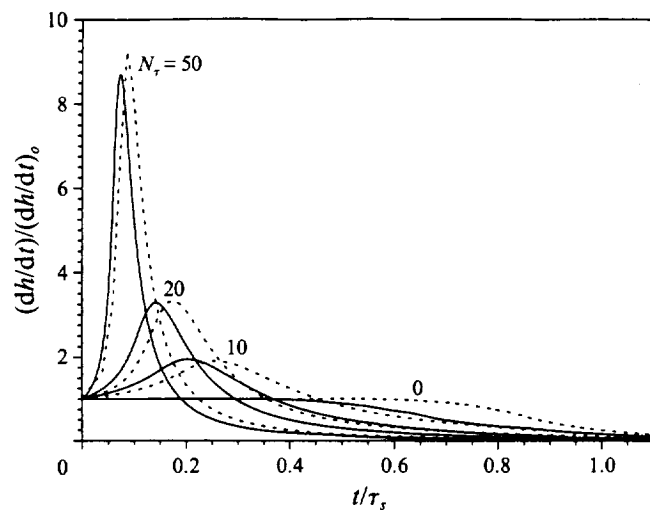

Fig. 3 - Predicted rate of phase separation versus time for a dispersion having $\hat{\mu} = 0.1$, $\hat{\sigma} = 0.2$ (solid lines), $\hat{\sigma} = 0.1$ (dashed lines), initial volume fraction $\phi_o = 0.05$, and different N_τ in a container of finite depth.
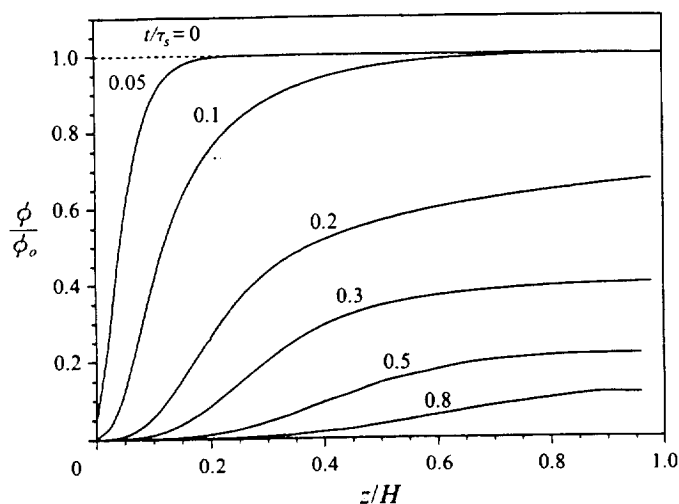

Fig. 4 - Predicted variation of volume fraction with position at different times for a dispersion having $\hat{\mu} = 0.1$, $\hat{\sigma} = 0.2$, and $N_\tau = 20$.
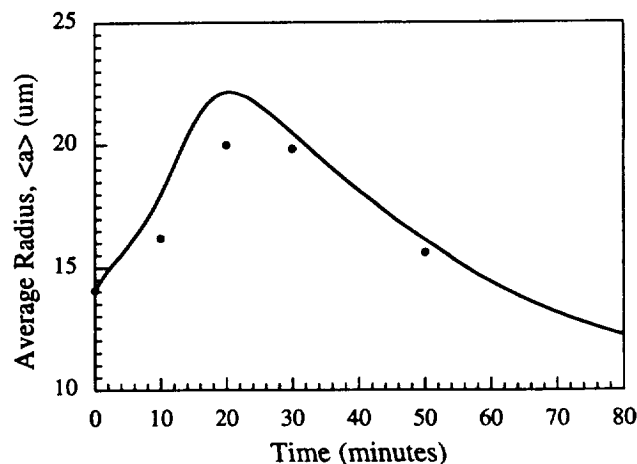

Fig. 5 - Evolution of the average drop radius at $z = 2.5$ cm for an initial dispersion of 3.4% by volume of 1,2-propanediol drops in a dibutyl sebacate matrix with 10.4 cm total height. The solid curve is the theoretical prediction and the solid circles are the experimental results.
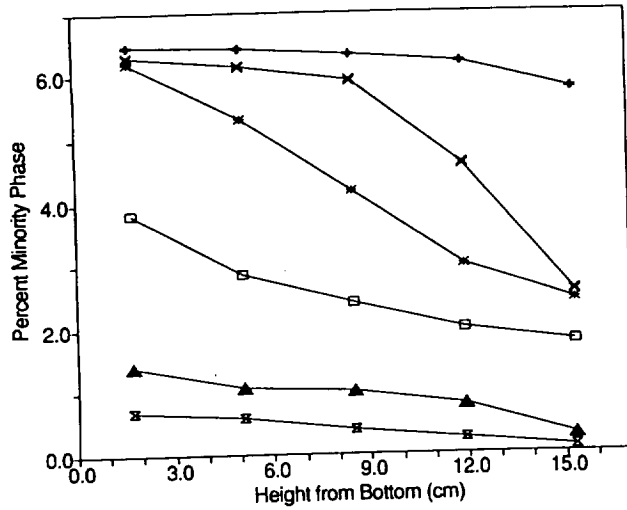
Fig. 6 - Volume percentage of dispersed phase versus distance from the bottom of the cuvette for dextran-rich drops at ϕ_o = 0.065 in a PEG-rich continuous phase with total height H = 17 cm, at t= 15, 30, 45, 60, 120, and 240 min (top to bottom).

Fig. 7 - The height of the lower phase versus time for an initial dispersion of 3.4% by volume of 1,2-propanediol drops in a dibutyl matrix with 14.5 cm total height; the filled circles represent the experimental measured data, the four solid curves represent the theoretical results with A = 5 × 10^{-15}, 5 × 10^{-16}, 1 × 10^{-17} erg, and 0 (no van der Waals forces), respectively, from top to bottom, and the dashed curve represents the results for no coalescence.
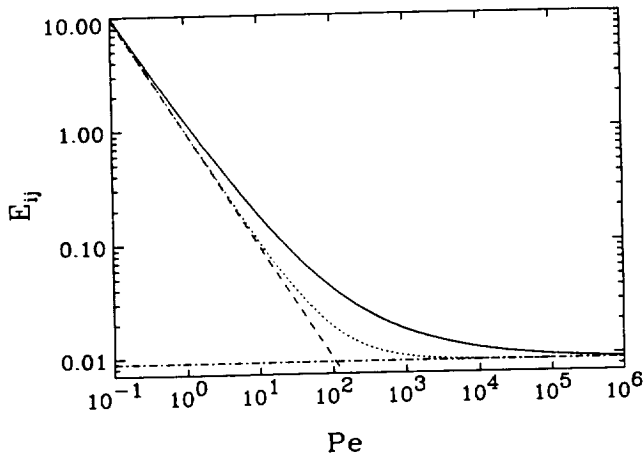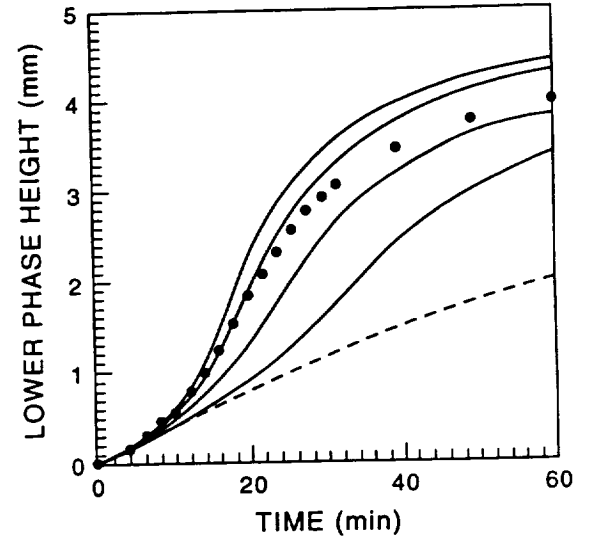

Fig. 8 - The collision efficiency as a function of the relative Péclet number for drops with size ratio λ = 0.25, viscosity ratio $\hat{\mu}$ = 10, and no interdroplet forces. The solid line represents the exact solution, the dotted line represents the additivity approximation, the dashed line is the Brownian collision efficiency, and the dashed-dotted line is the gravitational collision efficiency.

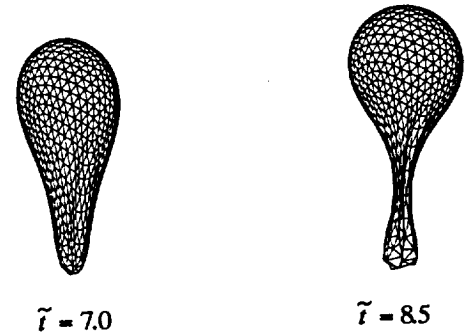$\tilde{t}$ = 7.0 $\tilde{t}$ = 8.5

Fig. 9 - Boundary-integral simulation of the stretching and impending breakup of a small drop by a larger drop (not shown) rising past it, for $\hat{\mu}$= 10^{-3}, a_2/a_1 = 0.7, and capillary number Ca = 0.72.

$\tilde{t}$ = 2.75 $\tilde{t}$ = 3.25 $\tilde{t}$ = 3.75
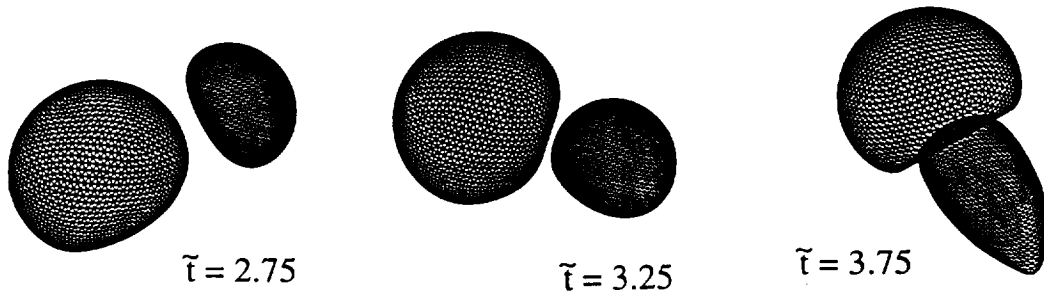
Fig. 10 - Boundary-integral simulation of the deformation-induced alignment of two rising bubbles with $\hat{\mu}$ = 10^{-3}, a_2/a_1 = 0.7, and Ca = 0.72.